Challenges in photon-starved space astronomy in a harsh radiation environment using CCDs

Conference or Workshop Item

Challenges in photon-starved space astronomy in a harsh radiation environment using CCDs

David J Hall*, Nathan Bush, Neil Murray, Jason Gow,
Andrew Clarke, Ross Burgon and Andrew Holland
Centre for Electronic Imaging, The Open University, Milton Keynes, MK7 6AA, UK

ABSTRACT

The Charge Coupled Device (CCD) has a long heritage for imaging and spectroscopy in many space astronomy missions. However, the harsh radiation environment experienced in orbit creates defects in the silicon that capture the signal being transferred through the CCD. This radiation damage has a detrimental impact on the detector performance and requires carefully planned mitigation strategies.

The ESA Gaia mission uses 106 CCDs, now orbiting around the second Lagrange point as part of the largest focal-plane ever launched. Following readout, signal electrons will be affected by the traps generated in the devices from the radiation environment and this degradation will be corrected for using a charge distortion model. ESA's Euclid mission will contain a focal plane of 36 CCDs in the VIS instrument. Moving further forwards, the World Space Observatory (WSO) UV spectrographs and the WFIRST-AFTA coronagraph intend to look at very faint sources in which mitigating the impact of traps on the transfer of single electron signals will be of great interest.

Following the development of novel experimental and analysis techniques, one is now able to study the impact of radiation on the detector to new levels of detail. Through a combination of TCAD simulations, defect studies and device testing, we are now probing the interaction of single electrons with individual radiation-induced traps to analyse the impact of radiation in photon-starved applications.

Keywords: CCD, radiation damage, defect, trap, CTE, Euclid, Gaia, WSO, WFIRST, mitigation

1. INTRODUCTION

The Charge Coupled Device (CCD) has many uses for both ground-based and space-based science applications. Prior to implementation as the focal plane imager or spectrometer for a space astronomy mission, the CCDs must undergo testing to determine their performance following time spent in orbit in the harsh radiation environment often encountered. Over the last few decades there has been a large amount of research undertaken into the study of radiation damage on CCDs. Whilst much is known about how the performance of the detectors will degrade over time following irradiation, there is still much to learn about the exact physical processes involved such as the precise defects formed within the silicon lattice and their impact.

Over more recent years, the science goals of space astronomy missions have become evermore demanding on the detectors used. Not only are the measurements required to be more precise, but the signal levels and signal level variations to be observed are getting smaller. The requirement for more precise, lower signal measurements presents an interesting area for research into the impact of the harsh radiation environment on the ability of the detectors to achieve the science goals of the missions. We must develop a deeper understanding of the physical processes behind the radiation-induced degradation in performance to both guide the mitigation studies before launch and enable the post-launch correction techniques. It is only with this fundamental understanding that we will begin to see the consequences of radiation damage on applications that require lower and lower signals and evermore precise measurements. In the next section we discuss a selection of missions in which understanding, and mitigating against, the radiation damage to the focal plane CCDs is of great importance.

*david.hall@open.ac.uk; phone +44 (0)1908 659 579; www.open.ac.uk/cei

2. OBSERVING LOWER SIGNALS IN SPACE ASTRONOMY

The European Space Agency's (ESA) Gaia mission was launched in late 2013 with the aim of charting a three-dimensional map of our galaxy [1]. The focal-plane array contained 106 e2v CCDs, creating an array totalling one billion pixels to catalogue one billion astronomical objects. Pre-launch testing of Gaia CCDs was carried out by Astrium (now Airbus Defence and Space), with data from Radiation Campaign 4 analysed at the Centre for Electronic Imaging at the Open University, UK, amongst several other institutions. This data analysis showed that signals averaging as low as one electron per pixel (equivalent to a GRVS = 15.75 spectrum) could be transferred through an irradiated Gaia Radial Velocity Spectrometer (RVS) [2] CCD under the Gaia operating conditions [3].

Euclid, ESA's mission to map the geometry of the dark Universe, is due to be launched in 2020 [4]. The Euclid Visible Instrument (VIS) will contain a focal plane of 36 e2v CCDs, each of 4k × 4k pixels, each 12 µm square [5-7]. Euclid VIS will perform weak gravitational lensing measurements, investigating shape changes in galaxies. Whilst not photon-starved, the high precision measurements needed for such a study require changes in signal of a few electrons to be measured; understanding the radiation damage impact with high certainty is therefore vital [8-9].

The World Space Observatory-Ultraviolet (WSO-UV) is a major international collaboration led by Russia. The mission aims to study the Universe in the 115-310 nm wavelength range, pushing beyond the reach of ground-based instruments [10]. The CCD camera system on board will be required to integrate for up to an hour and read out low signal levels with very low noise.

The Wide-Field Infrared Survey Telescope (WFIRST) is a NASA observatory that is designed to perform wide-field imaging and slit-less spectroscopic surveys of the near infrared (NIR) sky [11]. The WFIRST Astrophysics Focused Telescope Assets (WFIRST-AFTA) will aim to settle questions in exoplanet and dark energy research, advancing topics from galaxy evolution to planetary formation and structure [11]. The WFIRST-AFTA coronagraph instrument is currently baselined to use the Electron-Multiplying (EM) CCD [12]. The EM-CCD is similar to a standard CCD but includes an additional register, the gain register, that enables the multiplication of signal charge by impact ionisation. By increasing the signal before reaching the output node of the device, the signal is increased whilst the readout noise remains constant, thus effectively reducing the readout noise. With a readout noise level reducible to the sub-electron level, the EM-CCD is ideal for use in low-signal situations, however, in orbit the detector, as with all the detectors mentioned above, will undergo radiation damage that may have a major impact on the performance of the device.

3. RADIATION DAMAGE

When a CCD is used in the focal plane of a space astronomy telescope, it will find in orbit a harsh and unforgiving radiation environment. For many missions such as Gaia and Euclid, the radiation environment is dominated by high energy protons. These protons bombard the detector and can cause displacement damage in the silicon, disrupting the uniformity of the silicon lattice. We shall consider here only the effects in n-channel CCDs as these are the most common detector type for current space astronomy missions such as those discussed above. In reality, a similar process to that described below occurs in both n-channel CCDs (for signal electrons) and p-channel CCDs (for signal holes) [13-15].

When a high energy proton effectively knocks a silicon atom out of its lattice position, a vacancy (absence of a silicon atom) or vacancies are formed. The vacancy can diffuse through the lattice until it forms a stable defect, be that with another vacancy to form a divacancy or with a doping or impurity atom, such as phosphorous (Si-E) or oxygen (Si-A). Each defect creates a new energy level between the valence and conduction bands, forming a "trap" in the silicon. If signal electrons pass over a trap site with sufficient electron concentration, the trap can capture an electron. The captured electron will be released by the trap at a later time, with this time depending on the energy level of the trap and temperature of the device. The process of capture and release can be described using Shockley-Read-Hall theory [16-17] in which the capture and emission of signal electrons is described by capture and release time constants (τ_c and τ_e respectively) for each trap species, Equations 1 and 2, such that the probability of capture or emission can be described by Equation 3, where σ is the capture cross-section, n is the electron concentration, m_{dos} and m_c are the density of states and conductivity effective masses of the electron respectively, v_{th} is the thermal velocity, X is an entropy factor associated with the entropy change for electron emission from the trap and finally χ is a factor added to allow for any field enhanced emission affecting the trap emission time [18].

$$\tau_c = \frac{1}{\sigma n v_{th}} \tag{1}$$

$$\tau_e = \frac{1}{X\chi\sigma N_c v_{th}} \exp\left(\frac{E}{kT}\right) \tag{2}$$

$$P_x = 1 - \exp\left(-\frac{t}{\tau_x}\right) \tag{3}$$

As shown in Equations 1, 2 and 3, there are many parameters required to describe each trap species in the silicon. It is currently believed that there are five main traps that dominate in n-channel CCDs, Figure 1. The data shown in Figure 1 are based on literature studies and experimental testing over many years, with the literature values iterated towards the experimental data. These five energy levels, and the resulting five emission time constants at any given temperature, span over ten orders of magnitude in terms of the emission time constants and therefore any operating conditions that are chosen will find at least one traps species to be detrimental to performance.

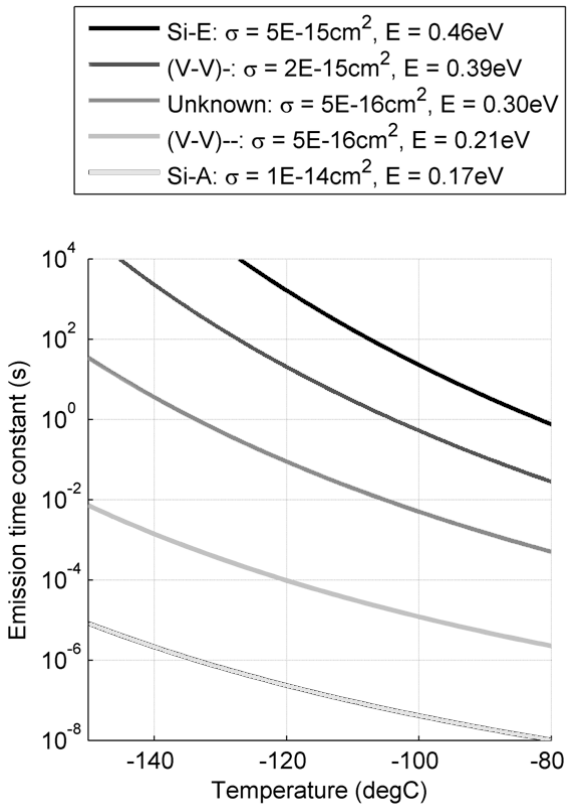

Figure 1. Trap species currently thought to dominate in n-channel CCDs following proton-irradiation.

It is only with a full understanding of each trap species present, and all the related parameters, that one can begin to fully appreciate the impact on the imaging and spectroscopy of a CCD in-orbit. As a result of many previous experimental studies, we are building an understanding of the trap species present in silicon after proton irradiation and can use this knowledge to develop mitigation techniques through novel operation modes and to help the correction of radiation damage effects that remain.

4. MITIGATION AND CORRECTION

In Section 3 we have introduced the theory of the damage caused by radiation to CCDs in space. Five trap emission time constants are shown in Figure 1 along with the associated energy levels (below the conduction band) and cross-sections. However, these results are based on an array of different data, taken from emission tails in CCD image data, charge transfer efficiency measurements and based heavily on literature results obtained through techniques such as Deep Level Transient Spectroscopy (DLTS). All of these techniques either observe a population of many traps in a piece of silicon (such as in DLTS) or observe the effect of many traps during readout through the CCD. In order to produce the most effective mitigation and correction strategies, it is vital to know about each trap species in much greater detail.

The most vital characteristics required are the number density of the traps in the device, the emission time constant at the temperature of operation and the capture cross-section (or probability of capture). It is also essential to combine this information, which is in itself interlinked, with knowledge of the charge storage geometry, that is, how the electron charge cloud is situated in the device, its volume and charge density. With this information it is possible to develop mitigation techniques to help reduce the effect of radiation damage on the images received from space and to develop effective correction algorithms to repair any damage to images that remains.

4.1 Mitigation techniques

Before the CCD is placed in-orbit, extensive research is required to determine the impact of radiation on the sensor's performance. As part of these studies, it is important to develop mitigation techniques that will minimise the impact of the radiation damage on the images that are to be taken with the aim of achieving the science goals of the mission. The precise operating conditions of the CCD, from temperature to clock timings, must be optimised to reduce not only the readout noise and dark current, but also the Charge Transfer Inefficiency (CTI). Several methods have been developed over recent years, primarily as part of studies for the Euclid mission, that enable the impact of radiation damage to be reduced. These methods do not change the inherent damage caused to the silicon lattice, but because of the understanding developed of how charge interacts with different trap species in the device, the impact of the traps can be reduced.

Studies in 2011 through 2012 by Gow *et al.* [8] and Hall *et al.* [19] investigated the impact of clock timings on CTI. The timings of interest were those of the transfer from electrode-to-electrode within a pixel, with the pixel-to-pixel timing fixed by the readout speed of the device. It was noted that for a three-phase readout register, "burst mode clocking", transferring charge quickly from phase 1 through 2 and 3 and back to 1 and hence maximising the sampling time for reduced readout noise, suffered from CTI that was approximately three time worse than that of "video mode" clocking, transferring charge with more even timings between electrodes. Using knowledge of the properties of the Si-A trap in silicon, this factor of improvement found with video mode over burst mode could be explained and a further optimisation achieved. A further improvement of over 20% was achieved through "even mode clocking", keeping the dwell time under each electrode the same. By keeping the charge as long as possible under each electrode and providing no faster transfers, the probability of any captured charge being released back into the charge packet from which it was captured is maximised, thus minimising the CTI under any set temperature and readout frequency.

Through an understanding of how charge is stored and transferred in a CCD, built up through use of Silvaco TCAD simulations [20-25], it is possible to "encourage" trapped charge to be emitted back into the charge packet from which it was captured, as detailed in Murray *et al.* (2013) [26]. In a standard device with equal width electrodes, and assuming traps are randomly distributed, if a charge packet passes from an electrode under which a trap is present to the neighbouring electrode (as part of the standard readout of the device) then if the trap emits in the required time period, there is a 50% probability that the trap will emit the capture electron back into the charge packet from which it was captured and 50% probability into the next pixel causing a charge tail to form. It is favourable, for reduced CTI, that the electron is emitted back into the charge packet from which it was captured such that there is no net loss of signal. Through a novel clocking method, in which several clock levels are used to shape the potential structure in the device, it is possible to reduce the number of traps that would result in deferred charge by a factor of two or more.

Through use of these, and other, mitigation strategies with carefully selected operating temperatures and readout frequencies, it is possible to manipulate the effect of capture and emission of signal by traps in the device. If a combination of mitigation strategies are appropriately combined, it can be possible to dramatically reduce the CTI without applying additional radiation shielding or orbital parameters. However, whilst the impact of radiation can be

reduced, some CTI effects will remain, and for this purpose it is necessary to develop appropriate correction algorithms to enable software post-processing corrections to be made to the images received from in-orbit.

4.2 Correction algorithms

In order to correct against the remaining charge loss and trailing caused by radiation damage in-orbit, it is possible to use post-processing, effectively "moving flux back to where it belongs" [27]. There has been extensive research into such corrections for the Hubble Space Telescope (HST), with the most recent improvements detailed in Massey *et al*. (2014) [27] and earlier work referenced there within. In summary, the images received from in-orbit are put through a charge transfer simulation, effectively adding further radiation damage effects that should ideally be identical to those in the device itself. Through an iterative process of adding further charge trailing and subtraction of successive images, it is possible to reduce the impact of the radiation damage on the image by up to 98% [27]. The ability of the process to correct the images is based very strongly on the ability of the simulation of charge transfer to accurately match that experienced in the devices in-orbit.

Moving forwards towards future missions, it is clear that the correction required is becoming evermore demanding. For Euclid, a 99% correction is required on CTI for the faintest galaxies towards the end of the mission [28]. In order to achieve this correction, more detail is required about the trap parameters and it is towards this aim that we discuss below the investigation of single defects and the charge storage geometry.

5. INVESTIGATING SINGLE DEFECTS

Whilst techniques such as DLTS can give a view of a population of traps, when we are observing small signals in a CCD, the precise interactions between an electron and each single trap becomes of vital importance. For large signals it is practical to consider the average effect of a population of traps, with the deferred charge tail allowing correction techniques to effectively recombine deferred charge with the original signals. However, when we consider a single electron being transferred, the notion of a deferred charge tail becomes meaningless. If a single electron is captured and later released then its position in the image will change with no evidence remaining of the original detection location. Therefore, as we approach the lowest signal levels, a deep and fundamental understanding at the single trap level is essential, both for guiding the development of mitigation techniques and for post-processing correction techniques.

In order to investigate single defects in the CCD a technique has been developed based on the pocket-pumping technique described in Janesick (2001) [29]. Using the technique of "trap-pumping" [30-31], so called because we are now considering individual traps rather than potential pockets, we can locate individual traps to the sub-pixel level and get a measure of their efficiency under the operating conditions of the device. The repeated transfer of a flat field of signal charge to the neighbouring pixel and back under the same clocking schemes as used in standard operation generates a high-low signal pair (a dipole) at the location of a trap, Figure 2 (left). The direction of the dipole (high-low or low-high) is determined by the position of the trap inside the pixel. The amplitude of the dipole provides an indication of the capture and release efficiency of each individual trap in the device and it is expected that this may provide an input to much more accurate correction algorithms in the future [30].

An alternative configuration of the trap-pumping technique, described in [32-34,14], allows the probing of specific trap parameters in the time domain. A flat field of signal is clocked back and forth between neighbouring pixels at a constant frequency, keeping the dwell time under each phase t_{ph} constant. Noting the amplitude of any dipoles in the image, each representing the location of a trap, one can then "pump" at a different clocking frequency (different t_{ph}) and repeat across a range of timings. In this way it is possible to scan the resonance of a trap in the time domain and gain a much fuller picture of the trap properties for each individual trap[1] that will impact the CTI of the device.

5.1 Number density of defects

Through the use of trap-pumping over a range clocking frequencies, with the possible addition of changing the temperature to speed up or slow down the emission time constants of a trap species, it is possible to determine the exact

[1] Provided that the radiation level is not so high that there are multiple traps per pixel. Some traps may require very low or very high clocking frequencies to enable the full investigation of their properties.

number of defects and their locations within the device. The peak resonance in the time domain for each dipole can be found such that the population of traps can be separated into a series of different trap species. For each species one can then determine the precise locations of any traps in the device. This information can feed directly into the mitigation strategies and the correction techniques described above.

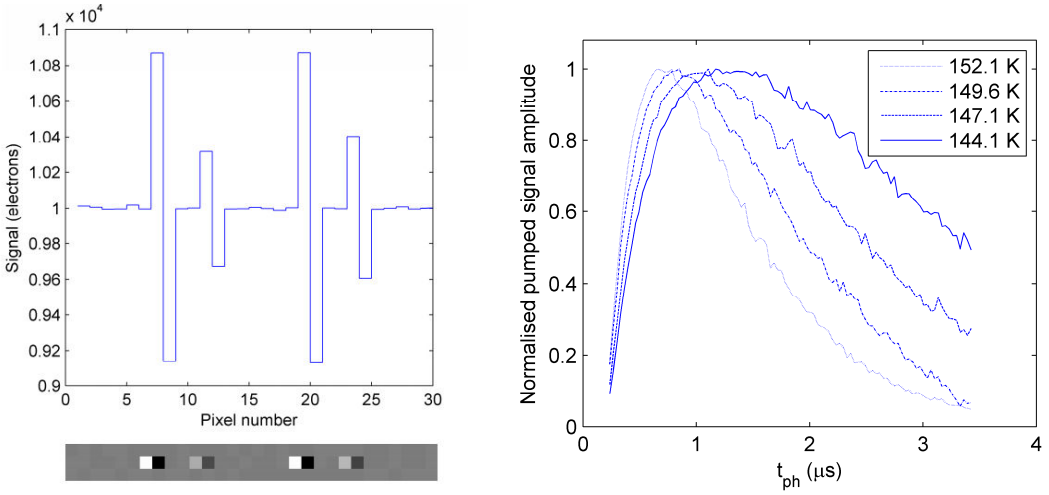

Figure 2. ***Left*****:** Example of the dipoles one might expect to see in the presence of traps in a CCD [33]. ***Right*****:** Resonance for a single trap, with each data point representing the amplitude of the dipole at the specified clock timing, shown across four temperatures [33]. The peak in the resonance curve at each temperature is given by the maximum of Equation 4, that being $t_{ph} = 2\ln(\tau_e)$, where τ_e is the emission time constant at the given temperature.

5.2 Emission time constants

For a given resonance curve of a trap, Figure 2 (right), the maximum value is given by the maximum value of the function shown in Equation 4, as derived in Hall *et al.* [32], where t_{ph} is the dwell time under each phase during pumping, τ_e is the emission time constant of the trap, N is the number of pumping cycles (number of transfers to neighbouring pixel and back to the start) and, to a first approximation, P_c is the probability of capture for the trap species.

$$I = NP_c\left(\exp\left(-\frac{t_{ph}}{\tau_e}\right) - \exp\left(-\frac{2t_{ph}}{\tau_e}\right)\right) \tag{4}$$

Equation 4 therefore gives a t_{ph} value for the peak of the resonance signal of $2\ln(\tau_e)$. The emission time constant can thus be found for each trap in a CCD and mapped across a range of temperatures to find the energy levels of the traps. In this way, a population of traps can be separated into the different species of traps present.

The results achieved so far using this method, tested on both n-channel and p-channel CCDs to probe electron and hole traps respectively, provide trap emission time constants with uncertainties of only a few percent [32-34,14]. Not only does this technique allow the properties of each trap to be determined independently, but it also allows a new level of detail to be examined in terms of the spread of emission time constants and energies for a population of what is believed to be the same trap species. A range of emission time constants of approximately one order of magnitude has been seen for what is believed to be a single trap species, such as that shown in Figure 3, with the reason for this variation still under investigation.

5.3 Capture dynamics

The resonance curves, as shown in Figure 2 (right), follow the form of Equation 4. The parameter P_c is, to a first approximation, the probability of capture for the trap in question. Through the fitting of this equation to the resonance

curve, one can investigate the capture dynamics of each individual trap in the CCD. Furthermore, by repeating the experiment at varying flat-field signal levels, one can determine the capture dynamics as a function of signal size. However, to fully understand the results obtained, one must first investigate the way in which the charge cloud sits within the CCD, how the electron density varies and how this affects the dynamics of charge capture by traps.

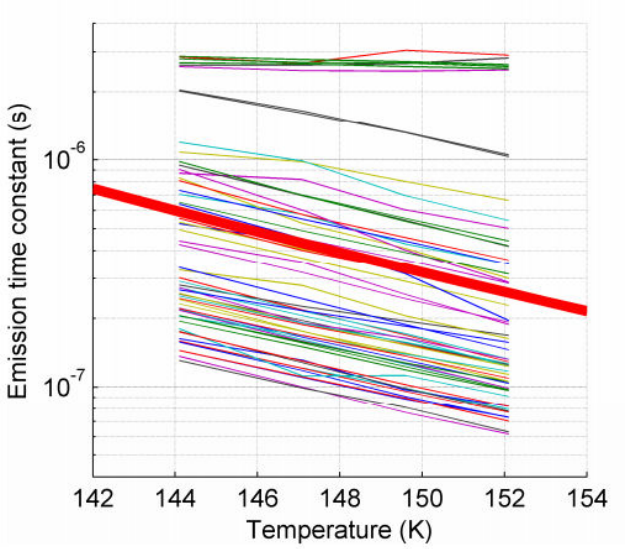

Figure 3. Emission time constants for a series of traps, all believed to be the Si-A, with each line representing the measurements at four different temperatures for one individual trap in the same device [33]. The lack of "zig-zagging" of the lines from one temperature to the next indicates that the spread in emission time constants is most likely a real effect and not due to uncertainties or systematic effects. The source of this variation is currently under investigation.

6. CHARGE STORAGE GEOMETRY

As discussed above, the charge storage geometry within the CCD will have a major impact on the CTI effects observed. The volume of silicon occupied by the signal charge with sufficient electron density for trapping to occur will determine the number of traps that the signal electrons will encounter as they pass through the device. Assuming a uniform distribution of traps in the silicon, the number of traps "seen" by the signal charge will scale linearly with the volume occupied (at sufficient electron density). Furthermore, the electron density at the trap location will determine the probability of capture, loosely defined in Equation 4.

Simulations have been carried out to investigate the charge storage characteristics in a variety of CCDs using Silvaco TCAD software [35] in three dimensions, with an example two-dimensional cut shown in Figure 4 (left). In order to achieve the best results possible, the simulations must include full processing information which has been obtained from e2v for the simulations detailed below through the collaborative link between e2v and the Open University. The simulations have been validated against experimental data where possible to give a level of confidence in the results presented.

Using the electron density simulated in Silvaco along with parameters gained from fitting Equation 4, it is possible to gain an indication of the location of each trap within the charge cloud. For example, if a trap has a high value for P_c at low signal levels then the trap is most likely to be found within the centre of the charge cloud. If a trap has a low value for P_c that increases slowly as the signal level increases then this trap is most likely to be towards the outer edges of the charge cloud.

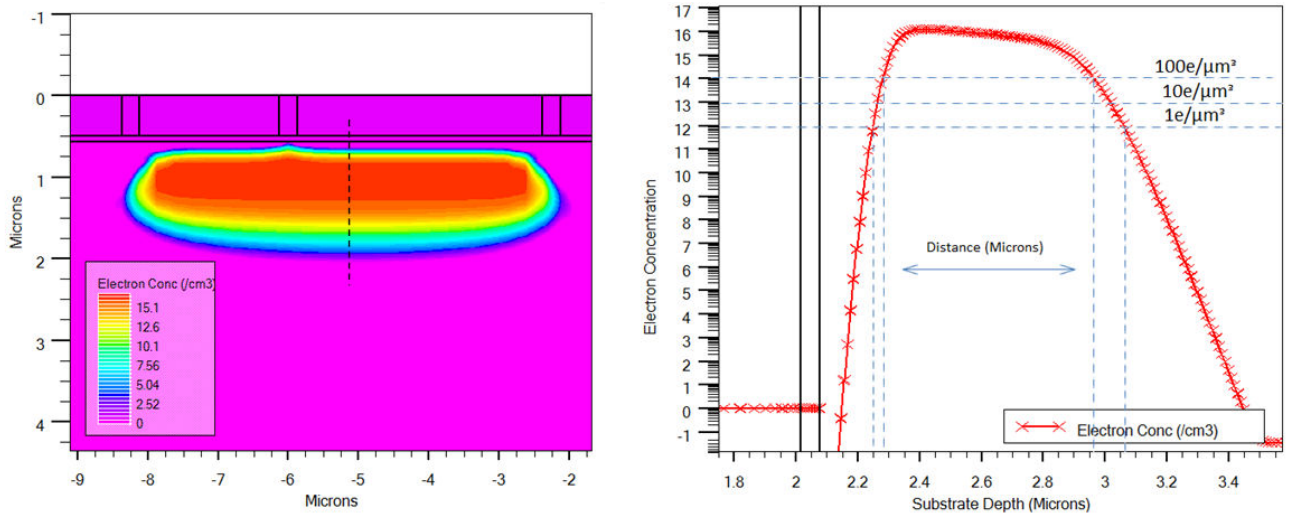

Figure 4. ***Left*****:** Cut through 3D Silvaco simulation of charge storage in a CCD [23]. ***Right*****:** One-dimensional profile through the left-hand charge storage simulation, showing the steep increase in density (noting the logarithmic electron density scale) [23].

In order to better represent the three-dimensional characteristics of the charge cloud, it would be favourable to be able to define the volume occupied by the signal (with sufficient electron density for trapping to occur) with a simple function. One such method to obtain a functional form for the charge storage variation with signal size is described in two papers by Clarke *et al.* (2012) and in Hall *et al.* (2012) [23-24,36]. For any given trap species and dwell time under an electrode, one can convert the electron density into a probability of capture using Shockley-Read-Hall theory (Section 3). In this way, it is possible to convert from electron concentration versus distance, as shown in Figure 4 (right), to the probability of capture versus distance. The sharp increases in electron concentration are exaggerated further still in probability space to give a relatively clear indication of trappable charge cloud size in each dimension. A simple cuboid model can then be created by multiplying the three dimensions, giving rise to the functional form shown in Figure 5.

Previous studies have modelled the resulting function through the use of a power law [37], such that the volume occupied varies with signal to the power β. In our own studies, however, we propose the use of an additional parameter to describe the specific behaviour observed at lower signal levels, Equation 5, where α, β and γ are all constants that will vary from one trap species and dwell time to another.

$$\text{volume "seen" by charge cloud} = \alpha\left(\text{signal}\right)^{\beta} + \gamma \tag{5}$$

In order to gain further trust in the simulations and the functional form of Equation 5, we have compared the raw function to experimental data, Figure 6, and run a Monte Carlo charge transfer simulation that makes use of the function for charge capture dynamics, Figure 7, as detailed in Hall *et al.* (2012) [23]. The consistency between the proposed functional form of Equation 5 and the experimental data gives confidence in the simulations and allows further analysis to be made of the impact of this functional form on radiation damage effects in CCDs.

One of the most fascinating insights that such modelling delivers is the impact of dwell time on the volume of silicon "seen" by the charge packet with sufficient probability of capture for charge to be lost to traps. As the dwell time increases, using Shockley-Read-Hall theory, the probability of capture increases such that the volume increases, Figure 5. When we discuss dwell time, we refer to the time spent by the charge packet in any one location. The integration time is therefore generally a period in which there is a very long dwell time (in relation to the transfer times during readout). For Euclid, for example, the integration time is several hundred seconds. For Gaia, the Time Delay and Integration (TDI) mode of operation means that any background signal will, on average, be present in approximately half the device at all times (the background will only sit under the electrodes that are "on" at any one time). We can use this information to explain why the presence of a low-level background signal can act to fill traps for much higher signals. During integration, or under TDI mode operation, the low-level background signals will fill traps in a volume that is larger than that in which they would fill traps during faster readout. Once the charge starts to be read out of the device,

the larger signals that are being transferred through the device see a smaller volume than that experienced during integration and the low-level background signals will have filled many of the traps that these signals encounter. It is important to note, however, that during a static integration, the background will only provide this shielding effect in the silicon under electrodes that are "on" during integration; the barrier phase traps will remain empty until a higher signal passes through them during readout.

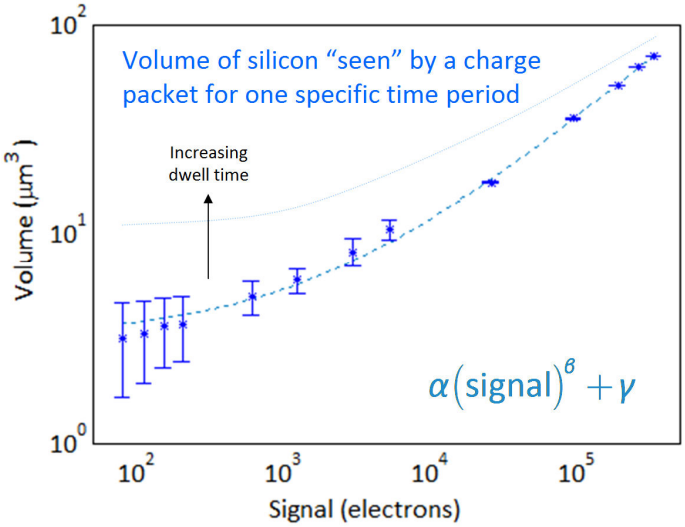

Figure 5. The volume of "trappable" signal within a pixel as a function of signal level, as described in the main text. The dashed line shows the volume for one trap species at one temperature and for one dwell time, with the functional form shown in the lower right equation. As the dwell time increases, the curve shifts upwards as indicated.

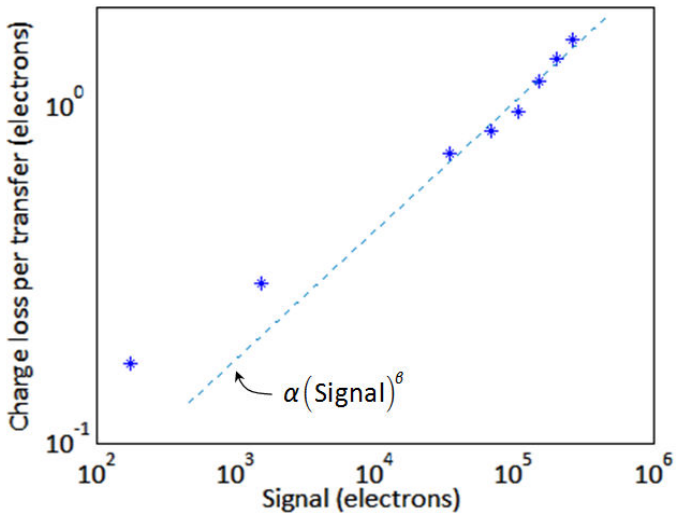

Figure 6. Charge loss per transfer for increasing signal levels. Experimental data from Extended Pixel Edge Response (EPER) data is shown by the points, with the functional form of a simple power law shown by the dashed line (i.e. without the additional γ parameter). The power law is insufficient to accurately map the functional form of the data and the γ parameter is required.

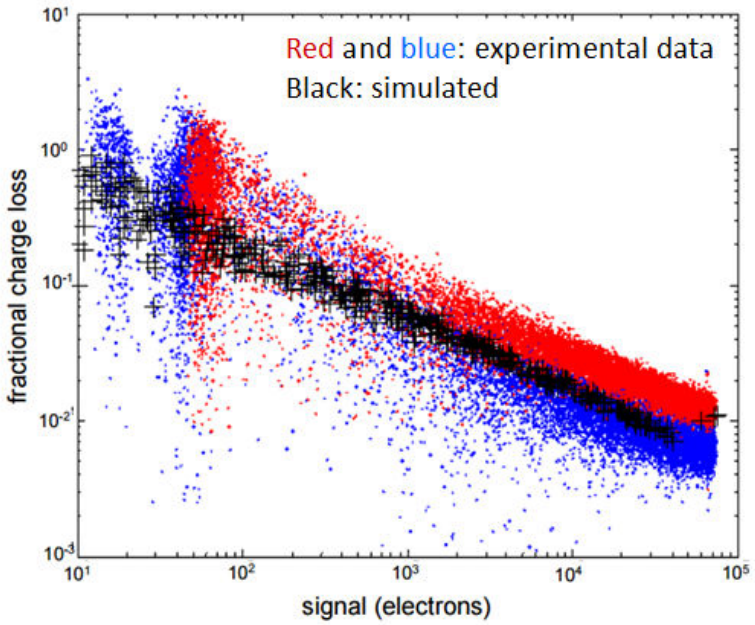

Figure 7. Fractional charge loss measurements (dots) from experimental data [38] at two different radiation levels of 8×10^9 and 1.6×10^{10} protons per cm^2 (50 MeV equivalent) compared to the Monte Carlo charge transfer simulation (black crosses) described in Hall *et al*. (2012) that uses the functional form shown in Equation 5, adapted from [23].

7. CONCLUSIONS

When the readout of large signals is affected by radiation damage, the smearing observed can be corrected through the techniques discussed in Section 4.2. However, for low signal levels, the process must be considered more carefully. Taking the signal down to the single electron level, one cannot then consider a single image to show an object being smeared against the direction of transfer through the CCD. A single electron will either make it through the device without being captured or it will be effectively moved in position through the process of capture and emission by a trap. In the case where the electron is trapped and emitted, it is only through the taking of many images that an image may begin to be reconstructed and an averaged "charge tail" allowed to form. It is therefore of greatest importance that all possible mitigation techniques are considered.

This is not to say that small signals cannot be transferred through a radiation damaged device. The results discussed in Section 2 from the pre-launch radiation studies for Gaia demonstrated that small signals, averaging less than one electron per pixel, could be transferred through the CCD, albeit for an extended "block" of signal and averaged over many frames. The results observed from the pre-launch testing for Gaia demonstrate the importance and significance of performing sufficient characterisation and optimisation before launch for any space astronomy mission using CCDs.

Further to the mitigation and correction strategies previously described, there are several additional options that might be considered. A Supplementary Buried Channel (SBC) can be added to the CCDs, similar to that used for the Gaia devices. The SBC effectively creates a very narrow channel with a small capacity through which small signals can be transferred. The smaller volume that is occupied by these small signals results in the signal "seeing" fewer traps and therefore suffering less from the radiation induced traps present in the main buried channel of the device.

Looking towards the future, studies are underway to investigate the properties of various silicon defect complexes, specifically looking for those that are formed more favourably than, for example, the Si-A [39-41]. This research, combining hybrid density functional theory with the trap-pumping studies described in Section 5, whilst in its early stages, has the potential to further improve mitigation against radiation-induced CTI through the use of isovalent doping.

Finally, it should be noted that the majority of studies undertaken in the literature are performed following room-temperature irradiations. Devices are often irradiated at room temperature and unconnected to the drive systems to be later cooled to the temperature of the mission and characterised for parameters such as CTI. In orbit, however, the situation is somewhat different. The device will usually be cold and running during the extended irradiation over the course of the mission. For this reason, we are moving towards the use of cryogenic irradiations, that is, to irradiate the device whilst running and cold, keeping the device cold from the point of irradiation until the testing is completed. This is of course a more complex procedure than the standard room temperature irradiation, but the results observed, such as in Gow *et al*. (2015) [42] and Murray *et al.* (2014) [13], suggest that this is an important change to be made to the test procedure to get a more realistic indication of the performance degradation that might be expected in-orbit.

8. ACKNOWLEDGEMENTS

With thanks to David Burt of e2v technologies for many years of discussion on the topic and the insight that he has provided, without whom this work would not have been possible.

REFERENCES

[1] L. Lindegren, C. Babusiaux, C. Bailer-Jones, U. Bastian, A. G. A. Brown, M. Cropper, E. Hg, C. Jordi, D. Katz, F. van Leeuwen, X. Luri, F. Mignard, J. H. J. de Bruijne and T. Prusti, "The Gaia mission: science, organization and present status", IAU Colloq., vol. 248, pp. 217-223, Jul. 2008.

[2] Katz, D.; Cropper, M.; Meynadier, F.; Jean-Antoine, A.; Allende Prieto, C.; Baker, S.; Benson, K.; Berthier, J.; Bigot, L.; Blomme, R.; Boudreault, S.; Chemin, L.; Crifo, F.; Damerdji, Y.; David, M.; David, P.; Delle Luche, C.; Dolding, C.; Frémat, Y.; Gerbier, N.; Gerssen, J.; Gómez, A.; Gosset, E.; Guerrier, A.; Guy, L.; Hall, D.; Hestroffer, D.; Huckle, H.; Jasniewicz, G.; Ludwig, H-G.; Martayan, C.; Morel, T.; Nguyen, A.-T.; Ocvirk, P.; Parr, C.; Royer, F.; Sartoretti, P.; Seabroke, G.; Simon, E.; Smith, M.; Soubiran, C.; Steinmetz, M.; Thévenin, F.; Turon, C.; Udry, S.; Veltz, L. and Viala, Y. (2010). Gaia spectroscopy: processing, performances and scientific returns. EAS Publications Series, 45 pp. 189–194.

[3] http://www.cosmos.esa.int/web/gaia/iow_20140114, accessed 22nd July 2015.

[4] R. Laureijs, et al. (2011, Oct). Euclid Definition Study Report, ArXiv e-prints 1110.3193 [Online]. Available: http://arxiv.org/abs/1110.3193.

[5] Cropper, Mark; Pottinger, S.; Niemi, S.-M.; Denniston, J.; Cole, R.; Szafraniec, M.; Mellier, Y.; Berthé, M.; Martignac, J.; Cara, C.; di Giorgio, A. M.; Sciortino, A.; Paltani, S.; Genolet, L.; Fourmand, J.-J.; Charra, M.; Guttridge, P.; Winter, B.; Endicott, J.; Holland, A.; Gow, J.; Murray, N.; Hall, D.; Amiaux, J.; Laureijs, R.; Racca, G.; Salvignol, J.-C.; Short, A.; Lorenzo Alvarez, J.; Kitching, T.; Hoekstra, H. and Massey, R. (2014). VIS: the visible imager for Euclid. In: Space Telescopes and Instrumentation 2014: Optical, Infrared, and Millimeter Wave, 22-27 July 2014, Montréal, Quebec.

[6] M. Cropper; S. Pottinger; S.-M. Niemi; J. Denniston; R. Cole; M. Szafraniec; Y. Mellier; M. Berthé; J. Martignac; C. Cara; A. M. di Giorgio; A. Sciortino; S. Paltani; L. Genolet; J.-J. Fourmand; M. Charra; P. Guttridge; B. Winter; J. Endicott; A. Holland; J. Gow; N. Murray; D. Hall; J. Amiaux; R. Laureijs; G. Racca; J.-C. Salvignol; A. Short; J. Lorenzo Alvarez; T. Kitching; H. Hoekstra; R. Massey, "VIS: the visible imager for Euclid", Proc. SPIE 9143, Space Telescopes and Instrumentation 2014: Optical, Infrared, and Millimeter Wave, 91430J (2 August 2014).

[7] Short, A. D.; Barry, D.; Berthe, M.; Boudin, N.; Boulade, O.; Cole, R.; Cropper, M.; Duvet, L.; Endicott, J.; Gaspar Venancio, L.; Gow, J.; Guttridge, P.; Hall, D.; Holland, A.; Israel, H.; Kohley, R.; Laureijs, R.; Lorenzo Alvarez, J.; Martignac, J.; Maskell, J.; Massey, R.; Murray, N.; Niemi, S.-M.; Pool, P.; Pottinger, S.; Prod'homme, T.; Racca, G.; Salvignol, J-C; Suske, W.; Szafraniec, M.; Verhoeve, P.; Walton, D. and Wheeler, R. (2014). The Euclid VIS CCD detector design, development, and programme status. In: High Energy, Optical, and Infrared Detectors for Astronomy VI, 22-27 June 2014, Montréal, Quebec.

[8] Gow, J. P. D.; Murray, Neil; Holland, Andrew; Hall, D. J. Hall; Cropper, M.; Hopkinson, G. and Duvet, L. (2012). "Assessment of space proton radiation-induced charge transfer inefficiency in the CCD204 for the Euclid space observatory". Journal of Instrumentation, 7 (C01030).

[9] Gow, J. P. D.; Murray, N. J.; Hall, D. J.; Clarke, A. S.; Burt, D.; Endicott, J. and Holland, A. D. (2012). "Assessment of proton radiation-induced charge transfer inefficiency in the CCD273 detector for the Euclid Dark Energy Mission". In: High Energy, Optical, and Infrared Detectors for Astronomy V, 1-6 July 2012, Amsterdam.
[10] http://www.wso-uv.org/, accessed 21st July 2015.
[11] http://wfirst.gsfc.nasa.gov, accessed 21st July 2015.
[12] L. K. Harding, R. T. Demers, M. Hoenk, B. Nemati, M. Cherng, D. Michaels, P. Peddada, A. Loca, N. Bush, D. Hall, N. Murray, J. Gow, R. Burgon, A. Holland, A. Reinheimer, P. R. Jorden, D. Jordan, "Technology Advancement of the CCD201-20 EMCCD for the WFIRST-AFTA Coronagraph Instrument: sensor characterization and radiation damage", JATIS (accepted subject to revisions, 2015).
[13] Murray, Neil J.; Holland, Andrew D.; Gow, Jason P. D.; Hall, David J.; Stefanov, Konstantin D.; Dryer, Ben J.; Barber, Simeon and Burt, David J. (2014). "Assessment of the performance and radiation damage effects under cryogenic temperatures of a P-channel CCD204s". In: High Energy, Optical, and Infrared Detectors for Astronomy VI, 22-27 July 2014, Montréal, Quebec.
[14] Wood, D.; Hall, D.; Murray, N.; Gow, J. and Holland, A. (2014). "Studying charge-trapping defects within the silicon lattice of a p-channel CCD using a single-trap "pumping" technique". Journal of Instrumentation, 9, article no. C12028.
[15] Nick J. Mostek ; Christopher J. Bebek ; Armin Karcher ; William F. Kolbe ; Natalie A. Roe ; Jonathan Thacker; "Charge trap identification for proton-irradiated p+ channel CCDs". Proc. SPIE 7742, High Energy, Optical, and Infrared Detectors for Astronomy IV, 774216 (July 16, 2010); doi:10.1117/12.855936.
[16] W. Shockley and W. T. Read Jr., "Statistics of the recombinations of holes and electrons", Phys. Rev., vol. 87, no. 5, pp. 835-842, Sept. 1952.
[17] R. N. Hall, "Electron-hole recombination in germanium", Phys. Rev., vol. 87, no. 5, pp. 387-387, Jul. 1952.
[18] G. R. Hopkinson and A. Mohammadzadeh, "Radiation effects in charge coupled device (CCD) imagers and CMOS active pixel sensors", Int. J. High Speed Electr. Syst., vol. 14, no. 2, pp. 419-443, Jun. 2004.
[19] Hall, David; Gow, Jason; Murray, Neil and Holland, Andrew (2012). "Optimisation of device clocking schemes to minimise the effects of radiation damage in charge-coupled devices". IEEE Transactions on Electron Devices, 59(4) pp. 1099–1106.
[20] Seabroke, G., Holland, A., Cropper, M., "Modelling radiation damage to ESA's Gaia satellite CCDs",Proc. SPIE, 7021 (2008).
[21] Seabroke, G., Holland, A., Burt D., Robbins, M., "Modelling electron distributions within ESA's Gaia satellite CCD pixels to mitigate radiation damage", Proc. SPIE, 7439 (2009)
[22] G. M. Seabroke, A. D. Holland, D. Burt, M. S. Robbins, "Silvaco ATLAS model of ESA's Gaia satellite e2v CCD91-72 pixels", Proc. of SPIE Astronomical Telescopes and Instrumentation (High Energy, Optical, and Infrared Detectors for Astronomy IV), 27-30 June 2010, San Diego, USA
[23] Hall, David J.; Holland, Andrew; Murray, Neil; Gow, Jason and Clarke, Andrew (2012). "Modelling charge transfer in a radiation damaged charge coupled device for Euclid". In: High Energy, Optical, and Infrared Detectors for Astronomy V, 01-06 July 2012, Amsterdam.
[24] Clarke, A. S.; Hall, D. J.; Holland, A. and Burt, D. (2012). "Modelling charge storage in Euclid CCD structures". Journal of Instrumentation, 7 (C0105)
[25] Clarke, A.; Hall, D.; Murray, N.; Gow, J.; Holland, A. and Burt, D. (2013). "Pixel-level modelling and verification for the EUCLID VIS CCD". In: UV/Optical/IR Space Telescopes and Instruments: Innovative Technologies and Concepts VI, 25-26 August 2013, San Diego, SPIE.
[26] Murray, Neil J.; Burt, David J.; Holland, Andrew D.; Stefanov, Konstantin D.; Gow, Jason P. D.; MacCormick, Calum; Dryer, Ben J. and Allanwood, Edgar A. H. (2013). "Multi-level parallel clocking of CCDs for: improving charge transfer efficiency, clearing persistence, clocked anti-blooming, and generating low-noise backgrounds for pumping". In: UV/Optical/IR Space Telescopes and Instruments: Innovative Technologies and Concepts VI, 25-26 August 2013, San Diego, SPIE.
[27] Massey, Richard; Schrabback, Tim; Cordes, Oliver; Marggraf, Ole; Miller, Lance; Hall, David; Cropper, Mark; Prod'homme, Thibaut and Matias Niemi, Sami (2014). "An improved model of charge transfer inefficiency and correction algorithm for the Hubble Space Telescope". Monthly Notices of the Royal Astronomical Society, 439(1) pp. 887–907.

[28] M. Cropper, H. Hoekstra, T. Kitching, R. Massey, J. Amiaux, L. Miller, Y. Mellier, J. Rhodes, B. Rowe, S. Pires, C. Saxton and R. Scaramella, “Defining a weak lensing experiment in space”, MNRAS, vol. 431, no. 4, pp. 3103-3126, Jun. 2013.
[29] J. R. Janesick, “Charge transfer” in Scientific charge-coupled devices, Washington: SPIE - The International Society for Optical Engineering, 2001.
[30] Murray, N. J.; Holland, A. D.; Gow, J. P. D.; Hall, D. J.; Tutt, James H.; Burt, D. and Endicott, J. (2012). “Mitigating radiation-induced charge transfer inefficiency in full-frame CCD applications by ‘pumping’ traps”. In: High Energy, Optical, and Infrared Detectors for Astronomy V, 1-6th July 2012, Amsterdam.
[31] Murray, Neil J.; Burt, David J.; Hall, David and Holland, Andrew D. (2013). “The relationship between pumped traps and signal loss in buried channel CCDs”. In: UV/Optical/IR Space Telescopes and Instruments: Innovative Technologies and Concepts VI,, 25-26 August 2013, San Diego, SPIE.
[32] Hall, David J.; Murray, Neil J.; Holland, Andrew D.; Gow, Jason; Clarke, Andrew and Burt, David (2014). “Determination of in situ trap properties in CCDs using a “single-trap pumping” technique”. IEEE Transactions on Nuclear Science, 61(4) pp. 1826–1833.
[33] Hall, David J.; Murray, Neil; Gow, Jason; Wood, Daniel and Holland, Andrew (2014). “In situ trap parameter studies in CCDs for space applications”. In: High Energy, Optical, and Infrared Detectors for Astronomy VI, 22-27 June 2014, Montréal, Quebec, p. 915408.
[34] Hall, David J.; Murray, Neil J.; Holland, Andrew D.; Gow, Jason; Clarke, Andrew and Burt, David (2014). Determination of in situ trap properties in CCDs using a "single-trap pumping" technique. IEEE Transactions on Nuclear Science, 61(4) pp. 1826–1833.
[35] ATLAS User’s Manual, “Device simulation software”, SILVACO Inc., 20th April 2010.
[36] Clarke, A.; Hall, D.; Murray, N.; Holland, A. and Burt, D. (2012). “Device modelling and model verification for the Euclid CCD273 detector”. In: High Energy, Optical, and Infrared Detectors for Astronomy V, 1-6th July 2012, Amsterdam.
[37] A. Short, C. Crowley, J.H.J. de Bruijne and T. Prod’homme, “An analytical model of radiation-induced charge transfer inefficiency for CCD detectors”, MNRAS, vol. 430, no. 4, pp. 3078-3085, Apr. 2013.
[38] Hopkinson, G., “Preliminary Test Report”, OA B E 0139435, revision 001.00, 12th February 2010.
[39] Londos, C. A.; Sgourou, E. N.; Hall, D. and Chroneos, A. (2014). “Vacancy-oxygen defects in silicon: the impact of isovalent doping”. Journal of Materials Science: Materials in Electronics, 25(6) pp. 2395–2410.
[40] Wang, Hao; Chroneos, Alexander; Hall, David; Sgourou, Efi and Schwingenschlogl, Udo (2013). Phosphorous-vacancy-oxygen defects in silicon. Journal of Materials Chemistry A, 1(37) pp. 11384–11388.
[41] H. Wang, A. Chroneos, C. A. Londos, E. N. Sgourou, and U. Schwingenschlögl, “A-centres in silicon studied with hybrid density functional theory”, Appl. Phys. Lett. 103, 052101 (2013)
[42] Gow, J. P. D.; Smith, P. H.; Pool, P.; Hall, D. J.; Holland, A. D. and Murray, N. J. (2015). “Proton irradiation of a swept charge device at cryogenic temperature and the subsequent annealing”. Journal of Instrumentation, 10(1), article no. C01037.